

Geometric Determinants of Directional Cell Motility Revealed Using Microcontact Printing[†]

Amy Brock,[‡] Eric Chang,[‡] Chia-Chi Ho,^{‡,§,||} Philip LeDuc,[‡] Xingyu Jiang,[§]
George M. Whitesides,[§] and Donald E. Ingber^{*,‡}

Vascular Biology Program, Departments of Pathology & Surgery, Children's Hospital/
Harvard Medical School, Boston, Massachusetts, and Department of Chemistry and Chemical
Biology, Harvard University, Cambridge, Massachusetts

Received August 12, 2002. In Final Form: October 25, 2002

Mammalian cells redirect their movement in response to changes in the physical properties of their extracellular matrix (ECM) adhesive scaffolds, including changes in available substrate area, shape, or flexibility. Yet, little is known about the cell's ability to discriminate between different types of spatial signals. Here we utilize a soft-lithography-based, microcontact printing technology in combination with automated computerized image analysis to explore the relationship between ECM geometry and directional motility. When fibroblast cells were cultured on fibronectin-coated adhesive islands with the same area (900 μm^2) but different geometric forms (square, triangle, pentagon, hexagon, trapezoid, various parallelograms) and aspect ratios, cells preferentially extended new lamellipodia from their corners. In addition, by imposing these simple geometric constraints through ECM, cells were directed to deposit new fibronectin fibrils in these same corner regions. These data indicate that mammalian cells can sense edges within ECM patterns that exhibit a wide range of angularity and that they use these spatial cues to guide where they will deposit ECM and extend new motile processes during the process of directional migration.

Introduction

Extracellular matrix (ECM) adhesive substrates play a central role in the establishment of normal tissue structure during embryogenesis.¹ For this reason, artificial ECMs and related biomaterials are currently being explored as structural scaffolds for tissue engineering applications.² Yet little is known about the determinants of ECM that are critical for control of the complex cell behaviors that underlie tissue development, such as directional cell motility. Recent studies suggest that physical cues from ECM, including local changes in substrate mechanics and shape, may provide important regulatory information to cells.^{1,3} However, exploration of this mechanical form of cell regulation has been limited by the lack of experimental techniques to control spatial interactions between cells and ECM.

Microcontact printing provides a versatile method to create novel adhesive substrates that are useful for spatially positioning mammalian cells and controlling their form and function.^{4–10} Adhesive islands of defined shape, size, and position on the micrometer scale may be

created with this soft-lithography-based technique on biocompatible substrates, such as glass.¹¹ Cells adhere preferentially to the islands that are coated with ECM adhesion molecules, such as fibronectin (FN), and not to the interisland regions on which nonadhesive poly-(ethylene glycol) (PEG) moieties are exposed. This system offers the opportunity to explore how simple structural cues, such as differently shaped adhesive substrates, influence more complicated biological responses which can be harnessed for cell and tissue engineering applications, including growth,^{4–7} differentiation,^{4,6} and apoptosis.^{4,8}

One of the most critical determinants of tissue form is directional control of cell migration. Examples include the oriented formation of capillary sprouts in the direction of a tumor³ and neural cell migration during formation of the nervous system in the embryo.¹² In mammalian cells, the initial step in cell migration is the formation of specialized, actin-rich membrane processes, known as lamellipodia and filopodia, that extend outward from the leading edge of the cell. The direction of lamellipodia extension can be modulated by soluble chemoattractants; for example, administration of a motility factor through a pipet induces lamellipodia extension from the closest region of the cell.¹³ Importantly, the surface characteristics of the terrain over which the cell moves also may influence

* To whom correspondence should be addressed. Donald E. Ingber, M.D., Ph.D., Vascular Biology Program, Departments of Pathology & Surgery, Children's Hospital—Harvard Medical School, Enders 1007, 300 Longwood Ave., Boston, MA 02115. Phone: (617) 355-8031. Fax: (617) 232-7914. E-mail: donald.ingber@tch.harvard.edu.

[†] Part of the *Langmuir* special issue entitled The Biomolecular Interface.

[‡] Children's Hospital/Harvard Medical School.

[§] Harvard University.

^{||} Current address: Department of Chemical Engineering, University of Cincinnati, Cincinnati, OH.

(1) Huang, S.; Ingber, D. E. *Nat. Cell Biol.* **1999**, *1*, E131–138.

(2) Mooney, D. J.; Mikos, A. G. *Sci. Am.* **1999**, *280*, 60–65.

(3) Ingber, D. *Circ. Res.*, in press.

(4) Singhvi, R.; Kumar, A.; Lopez, G. P.; Stephanopoulos, G. N.; Wang, D. L.; Whitesides, G. M.; Ingber, D. E. *Science* **1994**, *264*, 696–698.

(5) Chen, C. S.; Mrksich, M.; Huang, S.; Whitesides, G. M.; Ingber, D. E. *Science* **1997**, *276*, 1425–1428.

(6) Dike, L. E.; Chen, C. S.; Mrksich, M.; Tien, J.; Whitesides, G. M.; Ingber, D. E. *In Vitro Cell. Dev. Biol.: Anim.* **1999**, *35*, 441–448.

(7) Huang, S.; Chen, C. S.; Ingber, D. E. *Mol. Biol. Cell* **1998**, *9*, 3179–3193.

(8) Flusberg, D. A.; Numaguchi, Y.; Ingber, D. E. *Mol. Biol. Cell* **2001**, *12*, 3087–3094.

(9) Parker, K. P.; Brock, A. L.; Brangwynne, C. P.; Mannix, R.; Wang, N.; Ostuni, E. O.; Geisse, N. A.; Adams, J. C.; Whitesides, G. M.; Ingber, D. E. *FASEB J.* **2002**, *16*, 1196–1204.

(10) Thomas, C. H.; Lhoest, J. B.; Castner, D. G.; McFarland, C. D.; Healy, K. E. *J. Biomech. Eng.* **1999**, *121*, 40–48.

(11) LeDuc, P.; Ostuni, E.; Whitesides, G.; Ingber, D. *Methods Cell Biol.* **2002**, 385–401.

(12) Duband, J. L.; Dufour, S.; Yamada, K. M.; Thiery, J. P. *J. Cell Sci.* **1991**, *98*, 517–532.

(13) Bailly, M.; Yan, L.; Whitesides, G. M.; Condeelis, J. S.; Segall, J. E. *Exp. Cell Res.* **1998**, *241*, 285–299.

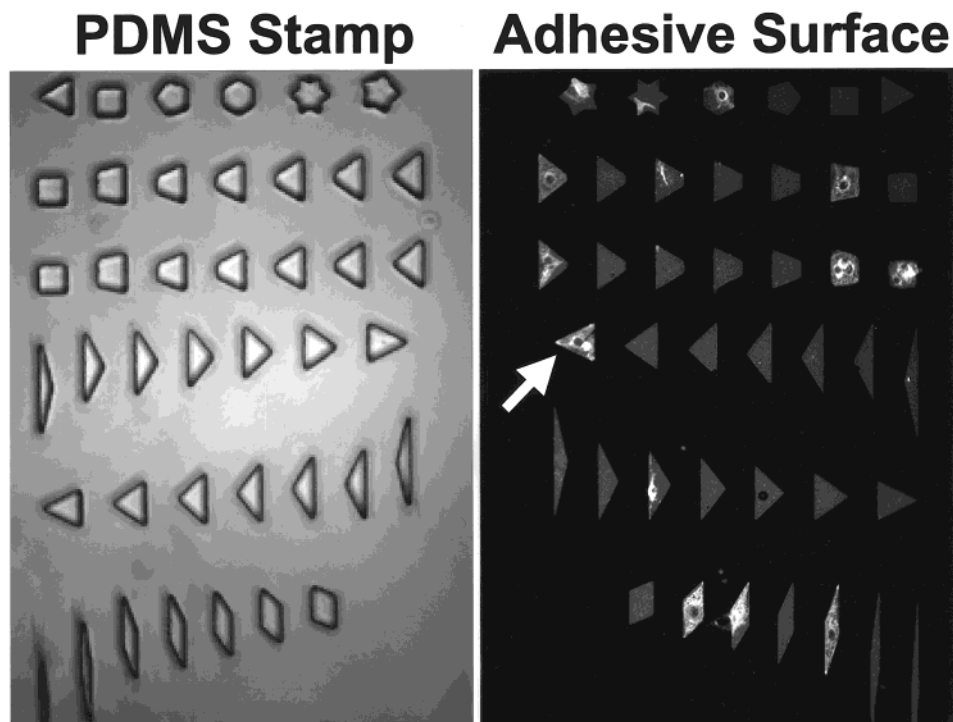


Figure 1. Low-magnification microscopic images of a phase contrast view of a PDMS stamp containing variously shaped islands of constant area ($900\ \mu\text{m}^2$) and of a fluorescent image of the FN-coated adhesive substrate created with this stamp using microcontact printing. The PDMS stamp (left), viewed here from below, was created by polymerizing the polymer against a silicon master with complementary surface topography. When this stamp was inked with alkanethiol and manually pushed down on a gold-coated cover glass, SAMs of hydrophobic alkanethiols formed only in the region where the polygonal mesas of the stamp contacted the planar substrate. The stamp was then removed, and the intervening areas of the gold-coated glass were covered with a second SAM composed of nonadhesive PEG-alkanethiol. When FN was added to the substrate, it adsorbed only to the hydrophobic polygonal islands. Thus, when FN is visualized by immunostaining, the evenly stained (gray) adhesive islands appear in a pattern that is nearly identical to that contained within the PDMS stamp, except that it is the mirror image because it is viewed from above (right). Note that the few quiescent cells that were cultured on this substrate in the absence of PDGF remain confined within the boundaries of the differently shaped adhesive islands. The arrow indicates a triangular island with an attached triangular cell that stains bright white; the adjacent island to the right in this view has no cell and stains bright gray.

the direction of migration. Cells cultured on a gradient of immobilized ECM protein migrate in the direction of increasing matrix concentration,¹⁴ and their migration velocity varies as a function of substrate stiffness.^{15,16}

We have recently shown that cells cultured on individual square FN islands created with microcontact printing preferentially extend lamellipodia and filopodia from their corner regions.⁹ Immunostaining and traction force microscopy revealed that square cells also localize focal adhesions and concentrate mechanical tension in these same areas.^{9,17} Thus, control of directional cell migration is sensitive not only to the concentration and composition of ECM protein but also to the geometry of the ECM-coated surface. In the present study, we explore in greater depth how cells respond to differently shaped adhesive substrates and how they discriminate between different geometric cues to more accurately define the spatial determinants of directional cell migration.

Results and Discussion

Micropatterned substrates containing an array of adhesive islands with the same area ($900\ \mu\text{m}^2$) but different

geometric forms (square, triangle, pentagon, hexagon, trapezoid, and various parallelograms) and aspect ratios were created using a soft-lithography-based, microcontact printing technique¹¹ (Figure 1). A pattern containing the polygons was designed using computer software and then printed to a mask. This mask was used to transfer the pattern to a thin layer of photoactive polymer (photoresist) which was spin-coated onto a silicon wafer via standard soft photolithographic techniques. A negative form of the pattern was then created from the topographical surface on the wafer by covering the surface with poly(dimethylsiloxane) (PDMS) followed by heat-induced polymerization. The flexible PDMS “stamp” (Figure 1, left) was peeled back from the wafer and coated with hydrophobic alkanethiols. The stamp was dried with an inert gas and then brought into tight contact with the surface of a cover glass containing a thin layer of deposited gold (with a thin titanium adhesion layer). The hydrophobic alkanethiol molecules are transferred only to regions of the glass surface that contact the raised regions of the stamp and, thus, that correspond directly to the polygonal island shapes. When transferred to the gold surfaces, these molecules self-assemble into a semicrystalline molecular monolayer or “self-assembled monolayer” (SAM) that is limited to the regions of the islands created on the original master. Next, a solution containing nonadhesive poly-(ethylene glycol)-alkanethiolate, which contains terminal triethylene glycol groups [$\text{HS}(\text{CH}_2)_{11}\text{O}(\text{CH}_2\text{CH}_2\text{O})_2\text{CH}_2\text{CH}_2\text{OH}$], was added to the patterned substrate. The nonadhesive alkanethiol self-assembles between the

(14) Bray, D. *Cell Movements*; Garland: New York, 1992; Chapter 2.

(15) Pelham, R. J., Jr.; Wang, Y.-L. *Proc. Natl. Acad. Sci. U.S.A.* **1997**, *94*, 13661–13665.

(16) Lo, C. M.; Wang, H. B.; Dembo, M.; Wang, Y.-L. *Biophys. J.* **2000**, *79*, 144–152.

(17) Wang, N.; Ostuni, E.; Ingber, D. E.; Whitesides, G. M. *Cell Motil. Cytoskeleton* **2002**, *52*, 97–106.

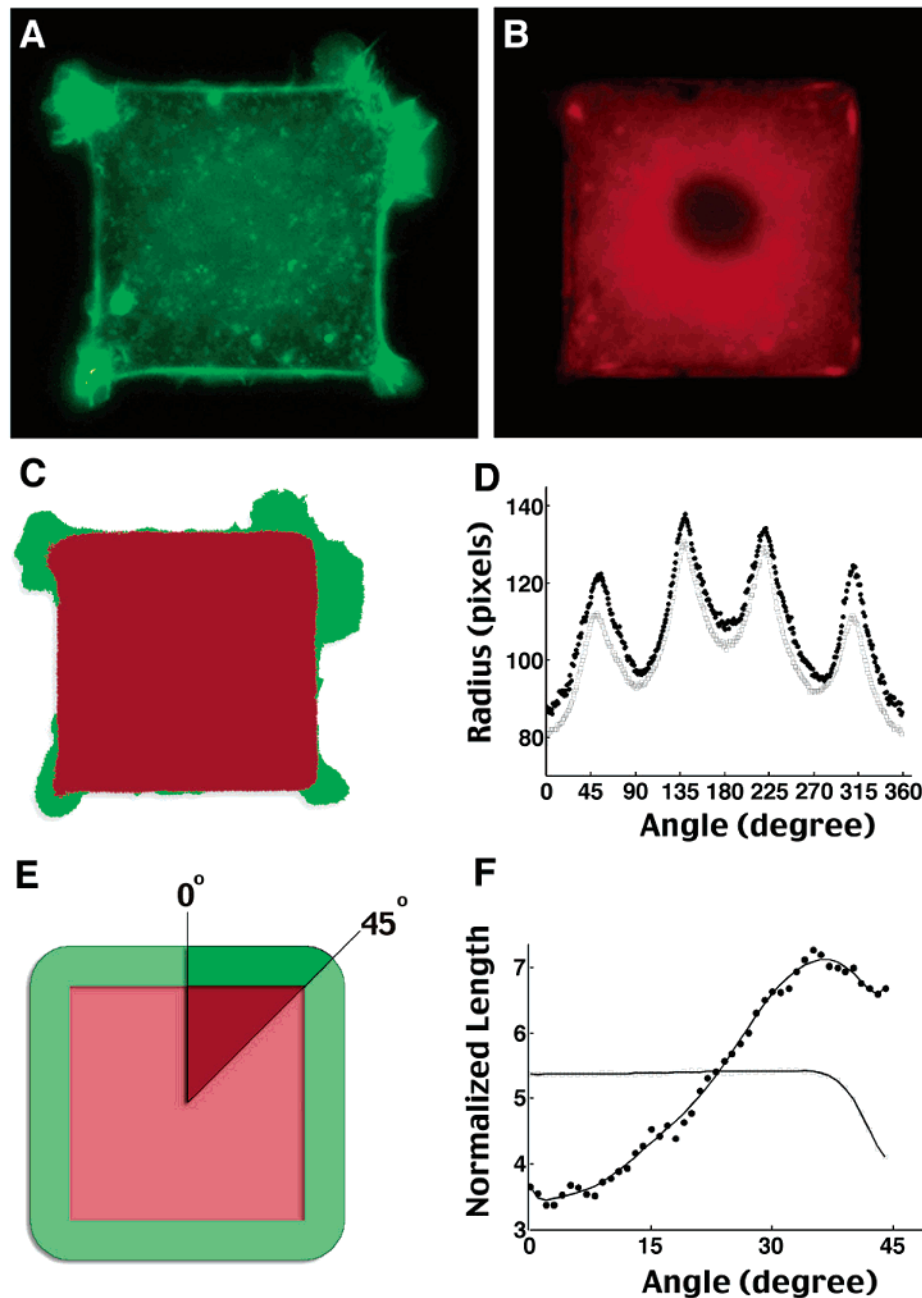


Figure 2. Geometric control of lamellipodia formation in cells on square adhesive islands. (A) Fluorescent microscopic images of a cell adherent to a square $30 \times 30 \mu\text{m}$ island that was stimulated with PDGF and stained for F-actin with fluoresceinated phalloidin. (B) The adhesive island beneath the cell shown in (A) after staining for FN using a rhodaminated secondary. (C) A schematic showing digitized images of (A) (green) and (B) (red) after being overlaid to visualize the localized distribution of new cell processes within the corner regions. (D) A plot of the radial distance from the centroid of each island to each point on the cell perimeter (solid circles) for multiple cells cultured on different square islands compared to the null hypothesis in which cell processes were assumed to extend equally at all points from the edge of the square island (open squares). Note that both the experimental data and theoretical results for the null hypothesis periodically peak every 90° in the regions that correspond to the corner of the square. However, there is also a relative increase in radial distance for the cell relative to the island in these same regions. (E) Schematic of the null hypothesis for the unbiased cell (green) relative to the FN square (red). In the case of square islands, all angles can be represented as multiples of the region swept out from 0° to 45° degrees due to symmetry, as highlighted in this schematic. (F) A plot of the length of processes that extend beyond the island perimeter for living cells (closed circles) versus that of the hypothetical unbiased cell (open squares) after normalization against the cosine of the respective angle for each radius. Note that specific geometric bias for lamellipodia extension from square fibroblasts is greatest between 33° and 45° , thus confirming that these motile processes preferentially extend from the corners of these cells.

hydrophobic SAM-covered islands, thus forming a continuous SAM over the entire substrate. A saturating concentration of the ECM molecule, FN, was coated on these substrates. The FN adsorbed only on the hydrophobic surfaces in the polygonal adhesive islands, while the intervening PEG-covered barrier regions remained uncoated (Figure 1, right) and hence nonadhesive.

When serum-deprived NIH3T3 fibroblasts were plated on the FN-coated micropatterned substrates, they preferentially attached to the islands and spread to assume the islands' size and shape (Figure 1). These quiescent cells remained constrained by the adhesive region and did not extend lamellipodia. In contrast, when cells adherent to square islands were stimulated with platelet-

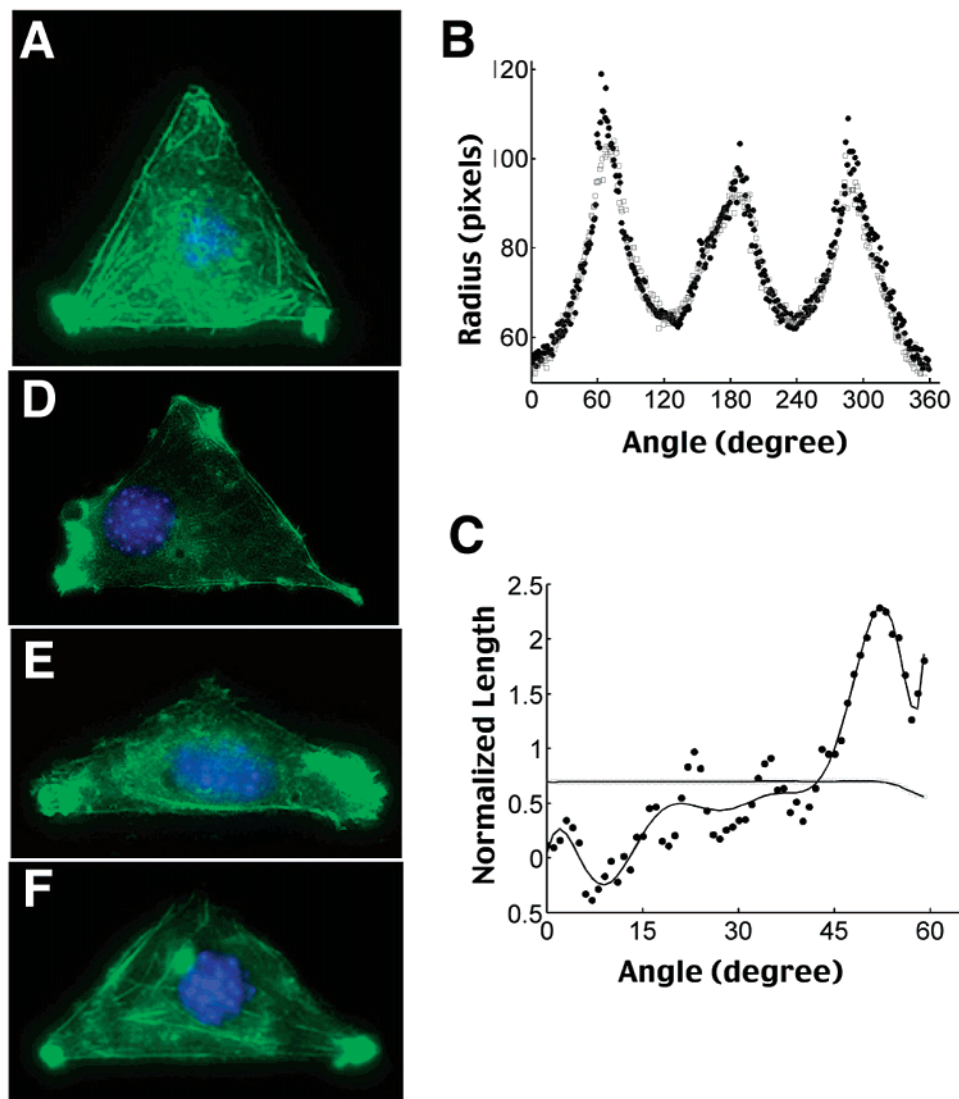


Figure 3. Geometric control of lamellipodia extension in cells on triangular islands. (A,D–F) PDGF-stimulated fibroblasts cultured on triangular islands with different aspect ratios and stained with phalloidin and DAPI to visualize F-actin (green) and nuclei (blue), respectively. Note that cells preferentially extend lamellipodia from the corner regions. (B) A plot showing the radial distance from the centroid of the triangular pattern to each point on the cell perimeter for the triangular cells (closed circles) compared to the unbiased null hypothesis (open squares). (C) A plot showing normalized extension lengths for the experimental cells (closed circles) versus a hypothetical unbiased cell (open squares) which demonstrates a clear bias for lamellipodia extension in the corner region, with a narrow peak between 50° and 60° .

derived growth factor (PDGF) to promote motility, the cells extended F-actin-rich lamellipodia and vertical membrane ruffles from their corner regions within 30 min of stimulation (Figure 2A). In a previous studies, we found that cells cultured on $30 \times 30 \mu\text{m}$ square islands preferentially extended motile processes from a region defined by $6 \mu\text{m}$ on either side of the 90° corner using a manual form of image analysis.⁹ However, that quantitation technique was limited only to use with square islands.

To investigate how cells discriminate between subtle geometric cues in a comprehensive way, we developed an automated computational technique for quantitation of lamellipodia extension that may be generalized for different island shapes and sizes. Briefly, fluorescent micrographs of the F-actin cytoskeleton (Figure 2A) and underlying FN-coated adhesive island (Figure 2B) were collected for each PDGF-stimulated cell. Only islands containing single adherent cells, as confirmed using DAPI staining, were used for this analysis. The images of fluorescent cells and islands were batch processed using

a boundary-detecting algorithm developed in Matlab. Thresholds for the boundaries outlining each cell and adhesive island were determined from histogram plots of pixel intensities for each condition. Binary images of the boundary edges were then generated and overlaid on one another; this process clearly delineated cell processes that extended past the edge of the adhesive island (Figure 2C). By use of this information, angles and radial distances were calculated from the centroid of each island to every pixel along the outer edge of the island and cell. The radial distances for each cell and pattern were then binned and averaged per degree of angular rotation around the centroid so that each cell contributes only one averaged radial distance per degree. The shortest radial distance to the edge of the island was used to register the angular phase of each cell/island pair. An average of all radial distances across the population of all cells and islands was then taken at each angle (Figure 2D).

In the case of the square cells, the period of the peak plotted in Figure 2D is 90° and each period is symmetric about a multiple of 45° . Thus the extension of the cells

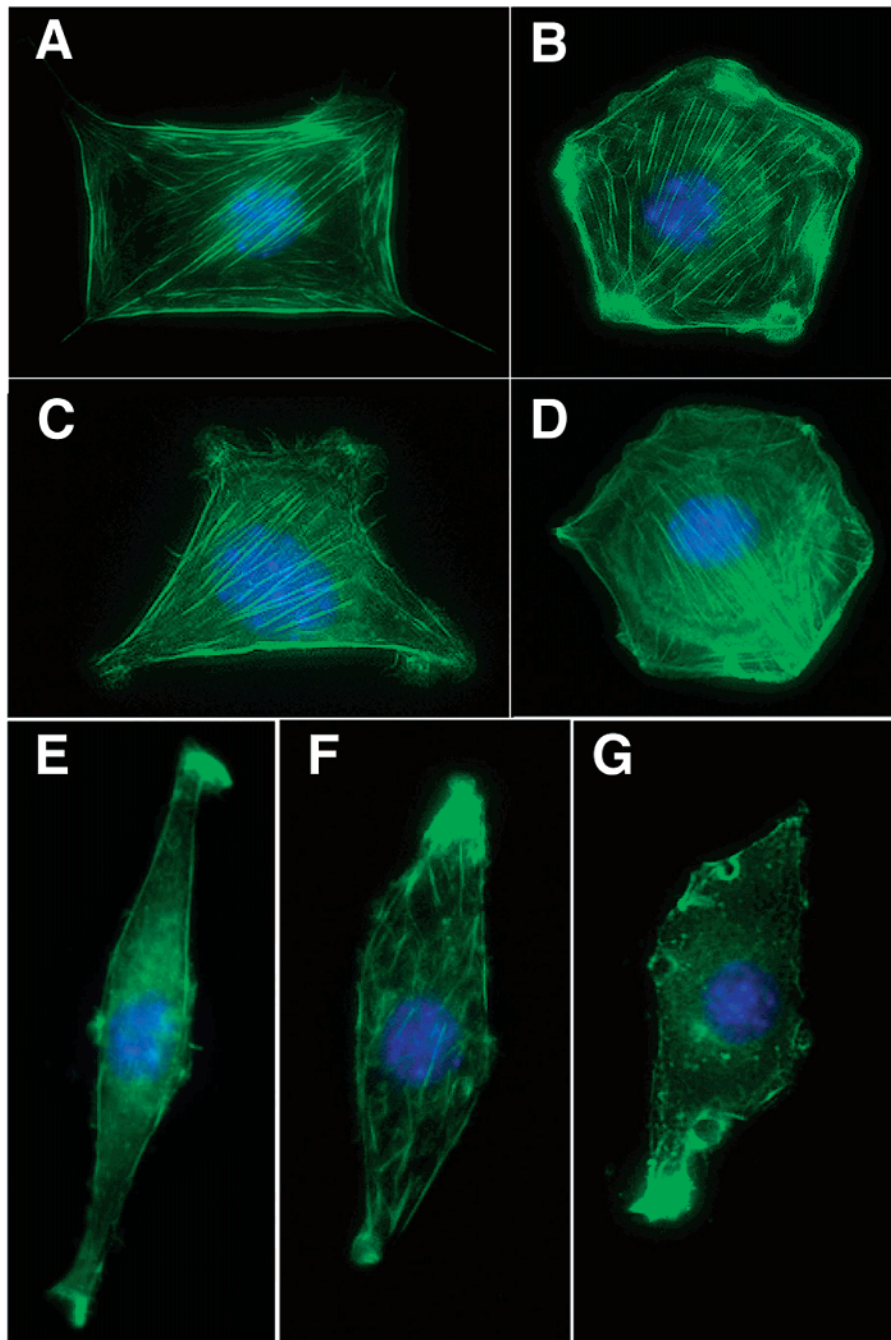


Figure 4. Directional lamellipodia extension in cells on differently shaped islands: (A) rectangle, (B) pentagon, (C) trapezoid, (D) hexagon, and parallelograms (E–G) of different aspect ratios and constant area ($900 \mu\text{m}^2$). All cells were stimulated with PDGF and stained with phalloidin and DAPI to visualize F-actin (green) and nuclei (blue), respectively. Note that lamellipodia were constrained to corners on all islands.

relative to the island edge (Figure 2C,D) can be clearly shown by plotting the difference in radial distance between the cell and the island at each angle between 0° and 45° (Figure 2E,F). Since the radial differences are measured angularly from the centroid, the radial differences were converted to Cartesian distances using the cosine of each radius's angle. Figure 2E is a schematic of the null hypothesis where a cell extends lamellipodia an equal distance from each point along the island perimeter. The null hypothesis was normalized to the cell such that the total area of the cell extending over the islands was the same in the null hypothesis case as in the experimental situation (e.g., green areas are equal in parts C and E of Figure 2). A plot of the normalized length of cell processes that extended beyond the island perimeter confirmed that

there was a specific geometric bias for lamellipodia extension from square fibroblasts. New motile processes formed preferentially in the corners relative to the sides, with the greatest increase in extension relative to the null hypothesis being observed between 33° and 45° , precisely in the corner regions of the square islands (Figure 2F).

To explore the generality of this technique, similar computerized analysis was then carried out using a data set for PDGF-stimulated cells cultured on FN-coated equilateral triangles of equal area ($900 \mu\text{m}^2$) to the squares (Figure 3A). In this case, when the radius along the periphery of the cell was compared to that of the triangular island, periodic peaks in cell radius occurred at 60° intervals, again with new cell extensions appearing

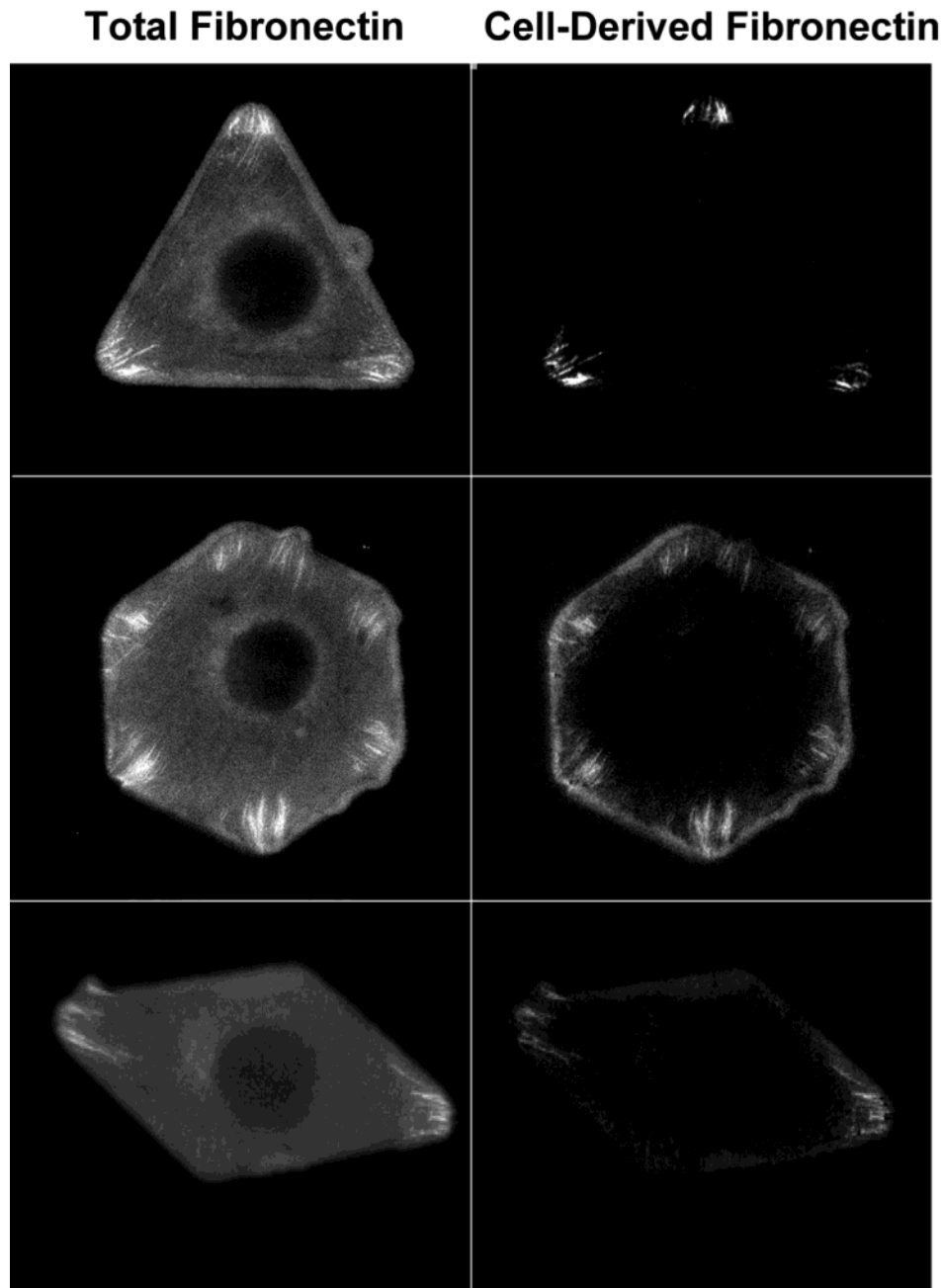


Figure 5. Cells deposit new FN fibrils in the corner regions of polygonal adhesive islands. (Left) Total FN staining within and beneath cells cultured for 24 h in serum-free medium on islands in the form of triangles (top), hexagons (middle), and parallelograms (bottom) visualized using anti-FN antibodies in conjunction with a fluoresceinated secondary. The islands were precoated with rhodaminated FN; however, this view reveals the pattern of both the immobilized FN and cell-derived FN. (Right) The same images as shown at the left after the rhodamine image for the immobilized FN was digitally subtracted to visualize newly deposited, cell-derived FN which appears in a fibrillar form precisely in the corner regions of each cell. Interesting, the hexagonal cell also accumulates FN fibrils in a seventh cell process where there appears to be a defect in the island shape that creates a seventh corner.

directly above the corners of the island (Figure 3B). As with the square cells (Figure 2), we observed a clear deviation between the angular dependence of the normalized extension length versus what would be expected for an unbiased cell (Figure 3C). Yet, the characteristic angle of lamellipodia extension from triangular islands differed from that observed in cells on squares: the radial length of the cell edge increased sharply between approximately 50° and 60° . Thus, the more acute angle of the triangle (60° versus 90°) appeared to more tightly constrain the region in which lamellipodia could form.

Preferential extension of motile processes from the corners was also observed in cells cultured on many different islands geometries, including triangles (Figure

3D–F), rectangles, pentagons, hexagons, trapezoids, and parallelograms of different aspect ratios (Figure 4A–G), but constant area ($900 \mu\text{m}^2$). These studies revealed that fibroblasts were able to extend lamellipodia from various angle sizes, ranging from acute angles of 15° to obtuse angles of 120° . In this study, however, cells appeared more likely to extend lamellipodia from acute angles (Figures 3E,F and 4E–G); extension from the obtuse angles was observed but occurred only rarely. These results are intriguing because previous studies of the cytoskeleton in motile cells have shown that the branched actin network grows through nucleation of new filaments at a fixed angle of 70° from the side of existing filaments.¹⁸ A number of actin-binding proteins¹⁸ and mRNAs¹⁹ also bind to specific

actin structures, such as filament intersection points or branch points with characteristic angles. Thus, spatial control of cell shape exerted at the micrometer scale by altering ECM island geometry apparently provides an experimental means to influence the local polymerization of actin and the structure of actin filament networks.

Past studies have shown that cells deposit new FN fibrils on the corners of square adhesive islands, directly beneath their focal adhesion sites where they exert greatest tractional forces.^{9,17} Adherent cells can remodel substrate-adsorbed FN by exerting cytoskeletal forces on their focal adhesion sites via integrin receptors.²⁰ However, cells also may deposit new FN and, in fact, many cells must continually synthesize and deposit their own ECM proteins in order to migrate.^{21,22} Thus, we set out to explore whether altering island geometry influences the position in which FN fibril assembly occurs, and we asked which mechanism is responsible for their production: reorganization of immobilized FN or new production by the adherent cells.

To determine whether FN fibrils were cell derived or the result of remodeling of immobilized FN that was precoated on adhesive islands, rhodamine-conjugated FN was adsorbed onto the micropatterned islands prior to cell plating. Cells adherent to triangular islands for 24 h were then stained for total FN using an antibody which recognizes both immobilized and cell-derived protein in conjunction with a fluoresceinated secondary antibody. A triangular island could be detected that had an even coating of FN over its entire surface and brightly stained, linear FN fibrils oriented radially within each corner (Figure 5 left). Subtraction of the rhodamine image from the fluorescein image resulted in an image that contained only the linear FN fibrils (Figure 5 right), thus indicating that these ECM proteins were newly synthesized and deposited by the overlying cell. Similar results were also obtained with cells adherent to hexagons and parallelograms (Figure 5) as well as other shaped islands.

It is important to note that these cells were not stimulated with PDGF and thus the constrained island geometry was sufficient to orient FN fibril assembly. Cells also form focal adhesions and apply greatest tensional forces in these regions.^{9,17} Thus, through this tension-driven mechanism, cells apparently are able to guide the deposition of new ECM proteins such that they are poised to rapidly extend lamellipodia and migrate along tension field lines (i.e., in the direction of greatest distortion or mechanical strain) when motility factors are administered.

One strength of the microcontact printing technology is its ability to provide structural cues at the size scale of individual cells that are able to trigger changes in the subcellular machinery such that specific structural rearrangements occur on the *molecular scale* within particular microdomains in the cell. The effects of adhesive island geometry on directional extension of lamellipodia is a clear example of this effect. The present data extend findings from past studies which demonstrate that cells can sense regions of the edge of the adhesive island that lose linearity and exhibit discrete angles. Moreover, cells respond to this break in linearity by reorienting their cytoskeleton, redirecting their tractional forces, depositing ECM fibrils, and extending lamellipodia all in the same direction (away

from the cell center). Our results also show that cells can discriminate between different angles and that more acute angles promote formation of narrower lamellipodia that are more tightly restricted to the corner of the island. These findings may help to explain how ECM guides cell migration during developmental processes, such as neurulation, where cells move on fibrillar tracks of FN²³ similar to those that promote acute angle formation at the cell periphery. The structural cues mapped out in this study also represent a first attempt at delineating design criteria for the fabrication of artificial ECMs that may be used to support, promote, or accelerate wound healing and tissue repair in the future. For example, incorporation of artificial adhesive scaffolds with microstructured surfaces that contain the correct geometric cues could provide a means to facilitate directional movement of cells during wound closure.

Experimental Protocol

Microfabrication of Adhesive Islands. Our detailed methods for microfabricating adhesive islands of defined size, shape, and position on the microscale have been published.¹¹ By use of this method, islands of constant area (900 μm^2) but different shape were created on gold-coated glass coverslips. The adhesive alkanethiol used in this study, hexadecanethiol, was purchased from Aldrich; the nonadhesive PEG-alkanethiolate was synthesized in our laboratory. After the micropatterned substrates were created by microcontact printing using the flexible stamp, the islands were coated with fibronectin (BD Biosciences) or rhodamine-conjugated fibronectin (Cytoskeleton, Inc.) (50 $\mu\text{g}/\text{mL}$ in phosphate-buffered saline) prior to use.

Cell Culture. NIH3T3 fibroblasts were passaged in Dulbecco's modified Eagle's medium (DMEM) supplemented with 10% fetal bovine serum, glutamine (0.3 mg/mL), penicillin (100 U/mL), streptomycin (100 $\mu\text{g}/\text{mL}$), 20 mM *N*-2-hydroxyethylpiperazine-*N*-2-ethanesulfonic acid (HEPES), and D-glucose (5 $\mu\text{g}/\text{L}$). Subconfluent cell monolayers that were serum-starved for 1 day were dissociated using trypsin-EDTA and plated (3000 cells/ cm^2) on micropatterned substrates in DMEM containing high-density lipoprotein (10 $\mu\text{g}/\text{mL}$), transferrin (5 $\mu\text{g}/\text{mL}$), and 1% bovine serum albumin. Lamellipodia extension was stimulated by the addition of 10 ng/mL PDGF (Sigma) for 30 min.

Immunostaining. At the end of each experiment, paraformaldehyde was added directly to the culture medium (final concentration of 4%) prior to washing to preserve the structure of lamellipodia; fixed cells were washed in phosphate-buffered saline (PBS) (Boston Bioproducts) and fixed for 15 additional min in 4% paraformaldehyde/PBS. Cells were permeabilized with 0.2% Triton X-100 in PBS prior to staining for F-actin, FN, and DNA (nuclei) using Alexa488-phalloidin (Molecular Probes), rabbit anti-FN antibody (Sigma), and DAPI (Sigma), respectively.

Computerized Morphometric Analysis. Immunofluorescence microscopy was carried out using a Nikon Diaphot 300 inverted microscope, and images of 41 different cells on square islands (164 corners) and 7 cells on triangular islands (21 corners) were acquired with the IP Lab Spectrum software package. Subsequent image analysis and quantitation of lamellipodia area were performed with Matlab version 6.1 (Mathworks) as described in Results and Discussion.

Acknowledgment. This work was supported by National Institutes of Health Grants CA-45548 (D.E.I.) and GM30367 (G.M.W.). We also thank the Harvard Materials Research Science and Engineering Center (MRSEC) for use of their microfabrication facilities and for salary support to P.L.

LA026394K

(18) Mullins, R. D.; Heuser, J. A.; Pollard, T. D. *Proc. Natl. Acad. Sci. U.S.A.* **1998**, *95*, 6181–6186.

(19) Bassell, G. J.; Powers, C. M.; Taneja, K. L.; Singer, R. H. *J. Cell Biol.* **1994**, *126*, 863–876.

(20) Ezell, R. M.; Goldmann, W. H.; Wang, N.; Parasharama, N.; Ingber, D. E. *Exp. Cell Res.* **1997**, *231*, 14–26.

(21) Madri, J. A.; Stenn, K. S. *Am. J. Pathol.* **1982**, *106*, 180.

(22) Wicha, M. S.; Liotta, L. A.; Vonderhaar, B. K.; Kidwell, W. R. *Dev. Biol.* **1980**, *80*, 253.

(23) Tucker, G. C.; Duband, J. L.; Dufour, S.; Thiery, J. P. *Development* **1998**, *103*, 81–94.